Optical Performance for the James Webb Space Telescope

Paul A. Lightsey*, Allison A. Barto, and James Contreras
Ball Aerospace & Technologies Corp., P. O. Box 1062, Boulder, CO 80631

ABSTRACT

The James Webb Space Telescope (JWST) is a large space based astronomical telescope that will operate at cryogenic temperatures, and utilizes a segmented primary mirror with active control. To achieve the science goals for JWST, the image quality over a wide spectral range is necessary. Several metrics related to the quality of the PSF have been used to capture the optical requirement to meet the science goals. We will present the requirements allocation from Point Spread Function Metrics to spatial frequency content in Wave Front Error allocations that reflect the unique forms associated with the active control aspects of the design.

Keywords: Point spread function, Strehl ratio, encircled energy, wave front error

INTRODUCTION

The James Webb Space Telescope (JWST) will be used for gathering science imagery and spectroscopy of astronomical objects within a spectral wavelength range from 0.6 μm to 27 μm. The ability to gather data for extremely faint sources within this spectral range is accomplished by a combination of a large collecting aperture telescope and operation at low cryogenic temperature shown in Figure 1. In addition to the having a large aperture for the radiometric sensitivity, the large aperture provides the underlying capability to achieve the desired spatial resolution at these wavelengths to gain scientific insight into the morphology of these distant faint astronomical objects. The wave front of the optical system will have the performance necessary to provide the point spread function (PSF) quality that supports the underlying spatial resolution of the large aperture.

The PSF as a complete measure of image quality is useful for simulating science data acquisition by convolution of the PSF with expected scenes. However, during the design, fabrication, integration, and testing of an optical system, simpler merit functions are often desired. There are a number of features of the PSF that lend themselves to being characterized by a simpler merit function. Some of these simpler single scalar number merit functions that have been used extensively in the past have been encaptured energy (encircled or ensquared), full width half maximum (FWHM), and Strehl ratio. William Wetherell[1] has pointed out that image quality analysis has been beset by "*unimania*" – the belief that highly complicated processes can be compared fully and accurately using a single one-real-number merit function. As a result, there has been an over reliance on these single value merit functions. To avoid this problem, the JWST requirements use a combination of single number metrics to collectively control different aspects of the PSF that affect the ability to achieve the desired science objectives. The point spread function metrics specified for JWST are the following:

Strehl Ratio > 0.8 at a wavelength of 2 μm
Encircled Energy Fraction > 0.74 at a wavelength of 1 μm
Strehl Ratio > 0.8 at a wavelength of 5.6 μm
Effective Anisotropy < 1% at a wavelength of 2 μm

In addition there are stability requirements that limit the variability of the Encircled Energy Fraction to less than 2% and the Effective Anisotropy to less than 0.1%.

Optical, Infrared, and Millimeter Space Telescopes, edited by John C. Mather,
Proceedings of SPIE Vol. 5487 (SPIE, Bellingham, WA, 2004)
0277-786X/04/$15 · doi: 10.1117/12.550091

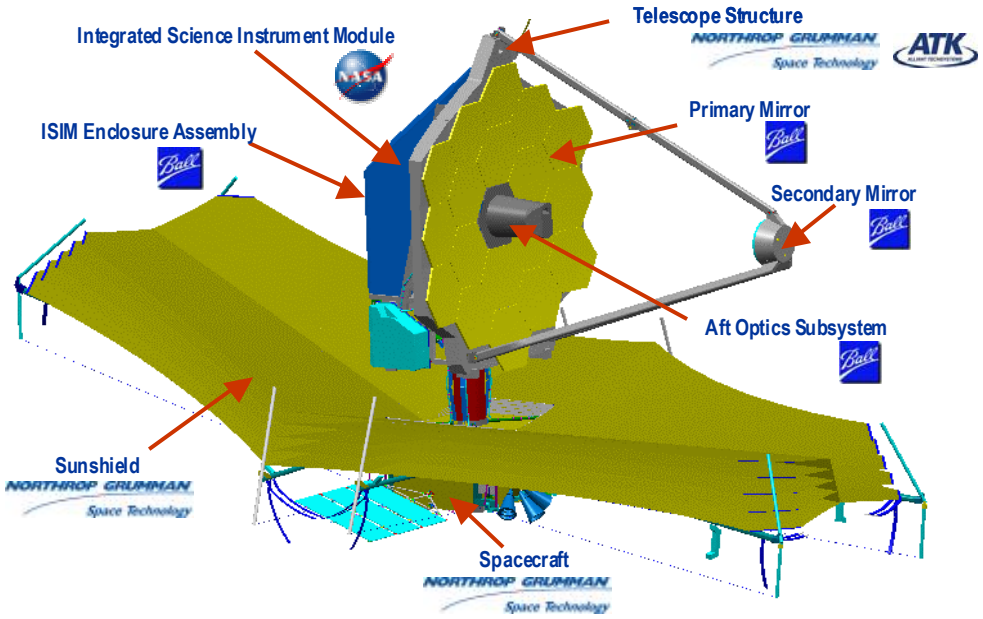

Figure 1. The JWST has a deployable telescope with the Primary Mirror having 18 actively controlled hexagonal segments and an actively controlled Secondary Mirror.

2. INTRINSIC APERTURE SHAPE DIFFRACTION

The large aperture (>25 m^2 clear aperture area) required for detecting extremely faint objects is implemented by relying on a stowed configuration for launch that is actively deployed and optically aligned after launch. The JWST architecture uses a segmented Primary Mirror (PM) and a deployable Secondary Mirror (see Figure 1). The PM uses a hexagonal tiling pattern for the segments. The diffraction pattern for a perfect hexagonal segmented aperture has been calculated[2] [3]. For small gaps (< 0.001 D), the diffraction from the gaps is quite small, and the PSF is dominated by diffraction from the serrated perimeter of the PM[4]. The "perfect" PSF from diffraction from the JWST aperture, including the secondary mirror support strut obscurations, is adequate. The principal task is to characterize the allowable WFE and image motion that are allowed before the PSF is degraded to where the specified metrics no longer meet the requirements.

3. RELATIONSHIP OF WFE TO PSF METRICS

The Strehl ratio is directly related to the total wave front error by the following relationship:

$$S = e^{-\left(2\pi \sigma_{opd}/\lambda\right)^2} \qquad \text{(eq. 1).}$$

Where σ_{opd} is the root mean square wave front error in units of optical path distance and λ the reference wavelength for the requirement. So, for example, the Strehl ratio requirement of 0.8 for JWST at a wavelength of 2 μm corresponds to a total WFE requirement of σ_{opd}=150 nm.

The image motion also affects the image quality, which is a time variation of the tilt of the WFE. The relationship between the Strehl ratio and the amount of image motion is given by

$$S_{im} = \left[1 + \frac{1}{2}\left(\pi \sigma_{im} D / \lambda\right)^2\right]^{-1} \qquad \text{(eq. 2).}$$

Where σ_{im} is the 1-axis rms image motion, D is the diameter of the aperture, and λ the reference wavelength for the requirement. The partitioning of the image motion allocation may then be expressed as an equivalent WFE calculated by

$$\sigma_{opd} = \left(\frac{\lambda}{2\pi}\right)\sqrt{\ln\left(\left[1+\frac{1}{2}\left(\pi\sigma_{im}D/\lambda\right)^2\right]^{-1}\right)} \qquad \text{(eq. 3).}$$

For JWST, the image motion errors are a result of a combination of un-rejected line-of-sight (LOS) errors from the Attitude Control System / Fine Guidance Sensor / Fine Steering Mirror (FGS/FSM) system, and internal structural dynamic responses to disturbances above the temporal control bandwidth of the ACS and FGS/FSM. The image motion budget also has allocations for image smear during an image exposure from a number of other effects that are not sensed and removed by the LOS control system.

The encircled energy fraction requirement controls the contribution to the WFE budget from mid and high spatial frequency errors. The motivation for this requirement is to control the amount of scattering/diffraction into the nearby region just beyond the central diffraction core. The ratio of the encircling radius and the dimension of the central diffraction core determine the spatial frequencies that affect the EEF performance. WFE at spatial frequencies below approximately 5 cycles/aperture (c/a) do not affect the EEF within a 150 mas radius at a wavelength of 1 μm.

The observatory architecture utilizes active six degree of freedom control of the PM segment positions, control of the PM segment radius of curvature (RoC), and six degree of freedom control of the SM. This provides active control of the low spatial frequencies up to nominally 5 c/a for a primary mirror (PM) architecture consisting of 18 hexagonal segments for the PM. The frequency demarcation for the encircled energy does not have a sharp transition. The error budget tracks separately the contributions below and above the control spatial bandwidth. This separates the critical uncompensated errors that affect the encircled energy from the total WFE that affects the Strehl ratio.

These higher frequencies are further separated into two domains to better describe the character of the WFE. These two domains are identified as mid frequency and high frequency. The mid frequencies are between the control frequency and 30 c/a. The high frequencies are those greater than 30 c/a. The mid frequency domain contains the control residual errors from the active positioning of the segments and control of their curvature. It also contains the fabrication errors on individual segments that are typically characterized by the low order aberrations at the segment level (up to approximately 6 cycles/segment). The allocations for the high frequency domain greater than 30 c/a account for residual figure errors on the optics including any "print through" of the underlying isogrid structure seen in the mirror surfaces (includes the secondary and tertiary mirrors), any patterns resulting from the polishing techniques, and the micro-roughness of the mirror surfaces. The active control of the surface for the semi-rigid and flexible segment mirrors reduces the errors at the actuator spacing frequencies and lower, but at the expense of inducing higher frequency "actuator print-through" distortions. Thus the effect of the active control is to reduce the overall WFE by lowering the low spatial frequency aberrations while adding to the mid and high frequency errors a lesser, but noticeable amount. The effect of this redistribution of the spatial frequency of the WFE makes it relatively easier to meet the Strehl (lower total WFE) but more difficult to achieve the EEF values (increased mid and high frequency errors). Figure 2 is a conceptual representation of the spatial frequency components of the WFE for JWST.

The stability requirement on the EEF is allocated by tracking separately the transient effects on the WFE budget. These capture transients ranging from effects occurring during time intervals corresponding to exposure-to-exposure intervals to those occurring over the longer time intervals between scheduled WFE maintenance operations.

There is also a requirement on the shape and stability of the shape of the PSF. This requirement given in terms of the effective anisotropy is sometimes referred to as the "ellipticity" requirement. The resulting PSFs based on the WFE and image motion budgets are analyzed to monitor design performance relative to this requirement. The non-isotropic forms of WFE within the budget correlate to the anisotropy performance.

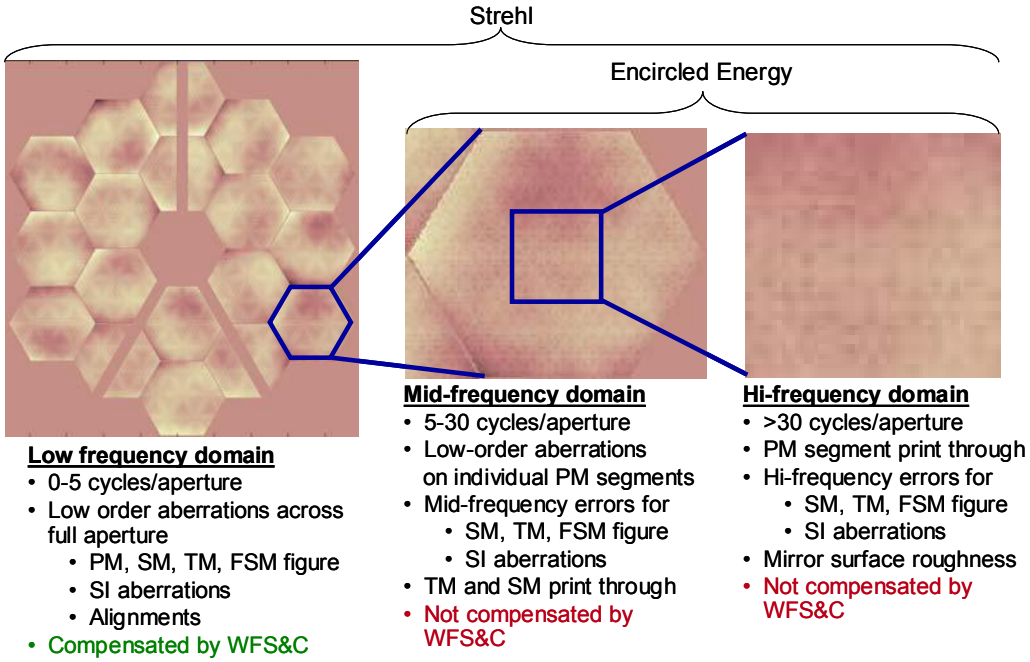

Figure 2. The spatial frequency contributions to the OPD

Figure 3 shows an example that captures the different aspects of the WFE budget. The individual blocks in the tree each contain a row with the allocation from the requirements, and a second row that tracks the current predicted performance at end-of-life for comparison. Each row has the total WFE and the break out of the total into the three spatial frequency bins. The total WFE tracks with the Strehl, and the combination of the mid and high track with the Encircled Energy. The example in Figure 3 also shows how a total allocation block for a given component may be further parsed out into three areas: "as-configured" WFE residual following Wave Front Control; image motion equivalent WFE; and WFE stability. The "as configured" corresponds to the as-built configuration (including the on-orbit cool-down and gravity release) plus the active compensation from the Wave Front Sensing and Control (WFS&C) process used during flight to adjust the alignment of the Secondary Mirror (SM) and the alignment and phasing of the PM to optimize the performance of the combined OTE/ISIM system.

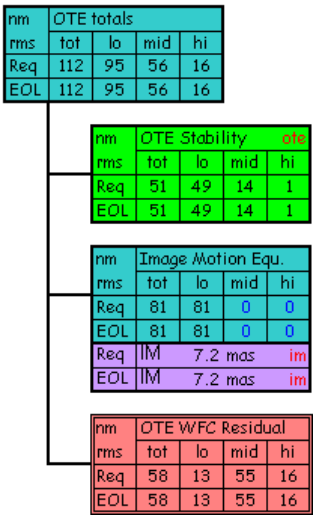

Figure 3. The allocations are partitioned into the "as configured" WFE following WFS&C, WFE equivalent for the image motion, and WFE stability

4. CONTRIBUTIONS FROM OBSERVATORY ELEMENTS

The top-level allocation is sub-allocated to the Optical Telescope Element (OTE) and the Integrated Science Instrument Module Element as shown in Figure 4. The latter is actually further subdivided between the WFE from the optical alignment tolerances for the integrating structure (ISIM Structure) and the specific Science Instrument (SI) channel for which the requirement applies. Note that there is a unique budget for each SI channel. One other allocation is shown at this top-level that is an artifact of using the NIRCam as the optical metrology instrument used to perform the on-orbit alignment and phasing of the telescope. This is referred to as the non-common path error. This is equivalent to the usual problem with ground alignments. The metrology process is typically calibrated so that the WFE artifacts may be extracted from the "raw" measured data to determine the WFE of the test piece, in this case the telescope. Since this data is used to adjust the telescope, any errors, or uncertainties in the calibration of the metrology instrument become transferred to the telescope. Thus, any uncertainties in the calibrated WFE of the NIRCam channel used for Wave Front Sensing will be interpreted as telescope WFE in the WFS&C process and be compensated by the transfer of the complementary error to the telescope, improving the performance in that NIRCam channel, but the added error to the telescope will increase the error in the telescope wave front presented to other SI channels.

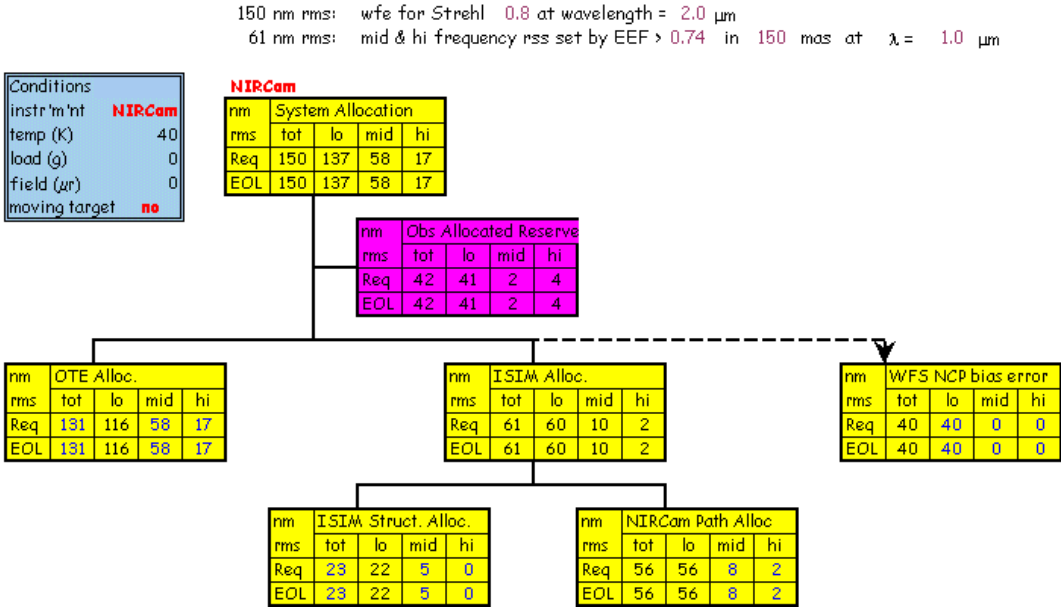

Figure 4. The System allocations are sub-allocated to the Optical Telescope Element (OTE) and the Integrated Science Instrument Module (ISIM). The ISIM allocation is explicitly separated into that for the science instruments, and that for the integrating structure alignment. The non-common path error is the undetected WFE in the WFS channel that is compensated by the OTE control, reducing the WFS channel error, but increases the error for the other SI channels.

5. CONTRIBUTIONS STRUCTURED BY SOURCE

Figure 5 shows the standard budgeting organization by source of error:

1) *Design Residual*: the allocation for the errors within the optimized design prescription, even if the system was built "perfectly".
2) *Alignment*: the allocation for tolerances in the inability to achieve perfect alignment of the elements relative to each other.
3) *Figure*: the allocation for the tolerances in the inability to produce the prescribed figure for each of the optical elements perfectly.

The fourth common category, "metrology", is included at lower levels of the budget structure to include metrology uncertainties used in the production/alignment processes.

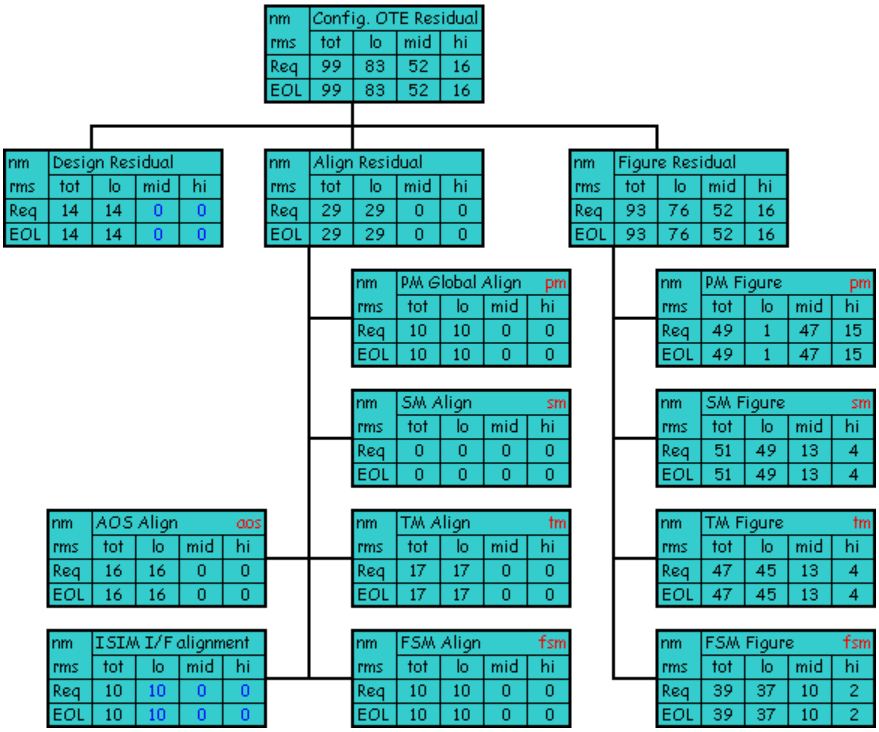

Figure 5. The errors are organized by design residual, the error that would occur if built perfectly, alignment residual from the inability to perfectly align the components relative to each other, and figure residual, the inability to figure the elements perfectly.

6. CONTRIBUTIONS ASSOCIATED WITH THE ACTIVE CONTROL PROCESS

The active degrees of freedom in the control process do two things: 1) correct rigid body positioning errors of the PM segments, SM position, and PM segment RoC., 2) and compensate low order wave front errors that are residual in the system. Figure 6 shows an example of the budget. The red block and purple boxes below it represent the WFS&C process. The purple box represents the mechanical tolerances for the commanding of each of the active control degrees of freedom the metrology errors for determining the magnitude of the commands. The metrology

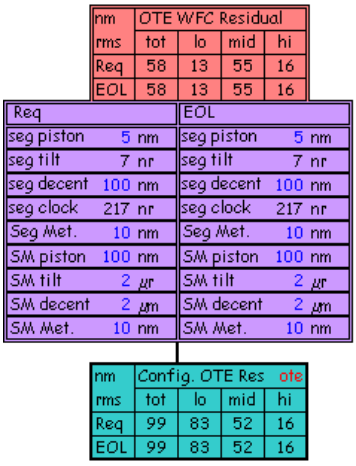

Figure 6. The active control command resolution and metrology errors are part of the residual errors following the active compensation of the low frequency errors. In addition, fitting errors for low frequency errors increase the mid frequency errors.

errors include algorithm accuracy limitations as well as sensor measurement errors. The resulting values in the red box are the residuals after compensation of the pre-WFS&C configuration errors by the WFS&C process. Recall that the degrees of freedom do not compensate the mid and high, and the low are not perfectly compensated due to metrology errors, commanding errors, and fitting errors. The fitting errors result from the fact that the 18 segments cannot necessarily fit smoothly a low order aberration. These fitting errors cause a small increase in the mid-frequency errors.

7. PM FIGURE ERRORS

Figure 7 shows the unique structure for the PM figure budget that accounts for the active positioning of the segments to the global parent surface and the separate figure allocations for the individual segments. Since the current architecture includes six degree of freedom control of the rigid body positioning of the segments, these errors will be corrected to zero. The metrology and commanding errors are accounted at the system level WFC box shown previously in Figure 6. However, there is a high frequency allocation, though small, that accounts for potential distortions in the mirror induced by the actuation mounting system.

The structure for the individual segment figure also has a unique structure to account for the active RoC control. Specifically, the allocations for curvature errors on each segment are tracked separately from the higher order aberrations that would be present on each segment. The active control process box accounts for the reduction of the curvature errors, while increasing the higher spatial frequency "induced distortion" from the mechanical stresses used to actively control the curvature of the segment surfaces. The amount of curvature error remaining is from the metrology error in measuring the amount of curvature to be corrected, and the command resolution error in the RoC control.

Though the active control of the curvature of each segment in principle could be used to compensate local "best-fit" curvature of other WFE contributors at each segment, we will take the conservative approach of not presuming any significant WFE reduction from this process. The correction of RoC errors of each segment from the parent surface is included in the PM figure budget.

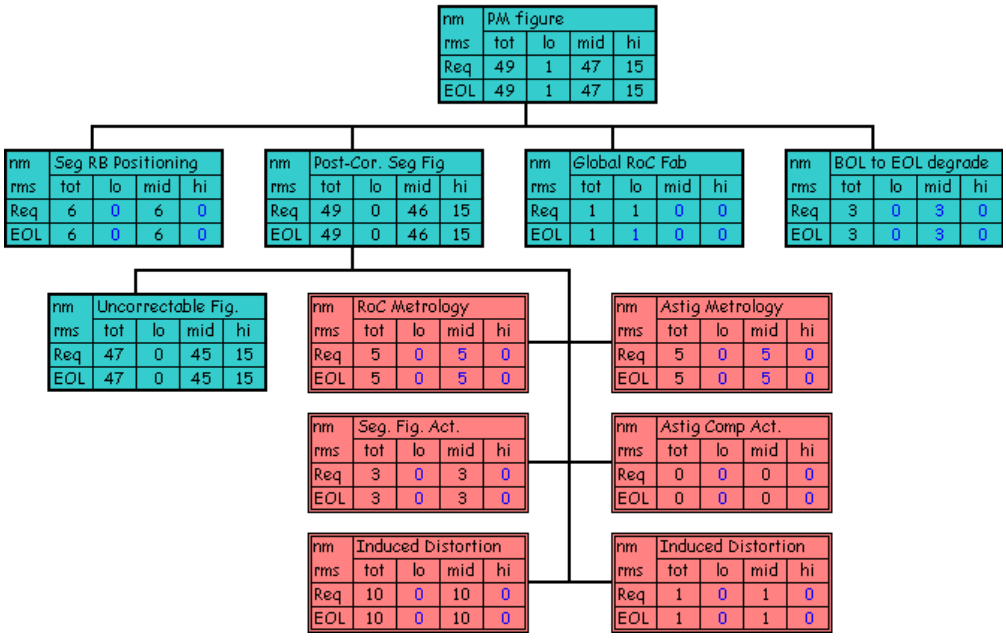

Figure 7. The PM figure budget shows the structure for the active rigid body positioning of the segments separately from the segment figure that includes active control of the radius of curvature of each segment.

8. STABILITY

The stability errors account for the variability in the image quality performance that occur between images and over time frames up to the intervals between WFS&C updates. These errors account for any structural changes that occur between the thermal extremes for pointing directions within the Field of Regard of the Observatory, slow structural "creep", and any potential transitory changes in the statistics for the dynamic effects. (For example, transitory effects that may change the standard deviation of the image motion.) The dominant contributor for the current architecture is anticipated to be the thermal stability of the structures. Figure 8 shows the budget structure for tracking alignment and figure stability errors.

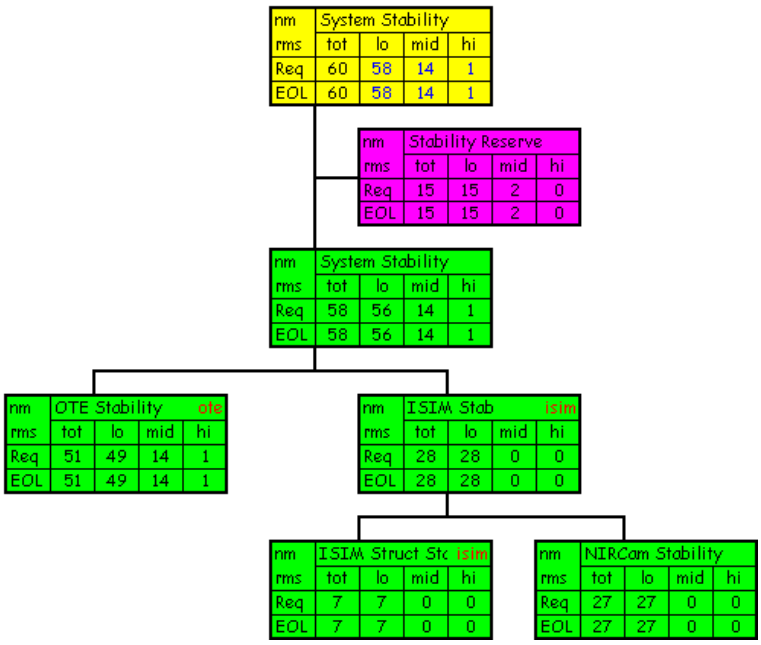

Figure 8. The transient allocations account for variability in the alignments and figure of the optical elements from changes in vibrational disturbances and thermal drifts.

6. SUMMARY

Large Space Telescopes by the virtue of their larger sizes offer increased resolution and signal gathering capabilities. However, these larger sizes also require deployment and active optical alignment and phasing after launch. The unique component features of such a system that collectively roll up to system image quality performance metrics have been assessed. The JWST optical system can provide the image quality required for the science objectives, but with a subtle difference from past experiences with smaller telescopes. This difference is the shift of the relative contribution to the WFE from the lower spatial frequencies into the higher frequency domains, putting more emphasis on Encircled Energy Requirements than Strehl.

REFERENCES

[1] Wetherell, W. B., *Applied Optics and Optical Engineering*, Vol. VIII, Chap. 6, Academic Press, New York, NY, 1980.
[2] Lightsey, P. A., Chrisp, M., "Image quality for large segmented telescopes", *IR Space Telescopes and Instruments,* **4850**, p. 453-460, SPIE, Bellingham, WA, 2003.
[3] Mast, T. S., Nelson, J. E., Welch, W. J., "Effects of primary mirror segmentation on telescope image quality", *International Conference on Advanced Technology Optical Telescopes*, **332**, p.123-133, SPIE, Bellingham, WA, 1982.
[4] Lightsey, P. A., Chrisp, M., "Image quality for large segmented telescopes", *IR Space Telescopes and Instruments,* **4850**, p. 453-460, SPIE, Bellingham, WA, 2003.